IMA Journal of Mathematical Control and Information Page 1 of 22
doi:10.1093/imamci/dnnxxx

Structure-preserving discretization and control of a 2D vibro-acoustic tube

NING LIU, YONGXIN WU, YANN LE GORREC
FEMTO-ST, Univ. Bourgogne Franche-Comté, CNRS, 24 rue Savary, F-25000 Besançon, France.
HECTOR RAMIREZ
Department of Electronic Engineering, Universidad Tecnica Federico Santa Maria, Avenida Espana 1680, Valparaiso, Chile
LAURENT LEFÈVRE
Univ. Grenoble Alpes, Grenoble INP, LCIS, 26000 Valence, France

This paper deals with the structure-preserving discretization and control of a 2D vibro-acoustic tube using the port-Hamiltonian framework. A discretization scheme is proposed and a set of precise basis functions are given in order to obtain a structure-preserving finite dimensional port- Hamiltonian approximation of the 2D vibro-acoustic system. Using the closed-loop structural invariants of the approximated system an energy-Casimir controller is derived. The performance of the proposed discretization scheme and the controller is shown by means of numerical simulations.

Keywords: Structure-preserving discretization, Control by interconnection, Vibro-acoustic system, Casimir invariant

1. Introduction

Based on the energy and a structured representation of the power flows and dissipation in the system, the port-Hamiltonian framework is particularly suited to describe the complex behavior of multi-physical systems [Duindam et al., 2009]. The port-Hamiltonian approach has been generalized to infinite-dimensional systems described by partial differential equations (PDEs) in [van der Schaft and Maschke, 2002, Le Gorrec et al., 2005]. From an application point of view, reduction of vibrations has drawn attention in both academic and industrial areas. Modeling and control of the vibro-acoustic systems have been investigated for different applications [Gardonio, 2002, Durand et al., 2008] in the last few years. The key point in these systems is the wave propagation process which can be modeled in a straightforward manner with the port-Hamiltonian framework. In [Trenchant et al., 2015], a port-Hamiltonian formulation of the 2D wave propagation has been proposed for a vibro-acoustic system on a rectangular spatial domain.

With the aim of simulating the system in a physically consistent way and furthermore the control design and implementation purpose, the numerical discretization scheme should preserve the Hamiltonian structure and the passivity of the original infinite dimensional system on the derived finite dimensional approximation. Research on structure-preserving discretization of port-Hamiltonian systems has drawn the attention of researchers in the last years and several methods, such as the ones based on mixed finite elements [Golo et al., 2004, Baaiu et al., 2009], pseudo-spectral [Moulla et al., 2011, Trang Vu et al., 2017], and finite volume have been proposed in [Kotyczka, 2016]. Recently an approach based on discrete exterior geometry has been proposed in [Seslija et al., 2012]. The general idea of these methods is to discretize the energy and co-energy variables using distinct low-order basis functions such that the

equations are exactly satisfied in these finite dimensional spaces.

In the 2D case, the authors in [Trenchant et al., 2017a, Trenchant et al., 2018a,b] have proposed to adopt the finite difference method to discretize the 2D port-Hamiltonian system on staggered grids. The finite volume method is employed to discretize 2D linear and non linear port-Hamiltonian systems in [Serhani et al., 2018]. The generalization of the discrete exterior geometry approach to the 2D case has been done in [Kotyczka and Maschke, 2017] on n-complexes. The mixed Galerkin discretization applied on the weak formulation of 1D and 2D port-Hamiltonian systems has been proposed in[Kotyczka et al., 2018]. The partitioned finite element method has been introduced in [Cardoso-Ribeiro et al., 2018] and also applied on the 2D plate models in [Brugnoli et al., 2019a,b].

A preliminary study of the structure-preserving discretization of a 2D vibro-acoustic system using a mixed finite element method has been proposed in [Wu et al., 2015]. In the present paper, we propose an discretized finite dimensional model with a precise choice of basis functions that satisfy the compatibility conditions associated with the discretization. Furthermore, an explicit finite dimensional input-output system is derived when considering the physical input and boundary conditions of 2D actuated vibro-acoustic system. In order to reduce/attenuate the wave propagation, an energy based control method based on closed-loop structural invariants similar to the on proposed in [Trenchant et al., 2017b] is investigated. By using this method, we can shape the energy function in the closed loop system to the desired one with a specific conservative boundary interconnection.

This paper is structured as follows. The infinite dimensional port-Hamiltonian system is recalled in Section 2 and then applied on the 2-D vibro-acoustic system which is obtained from the 3-D model with a geometry reduction [Trang Vu et al., 2019]. Section 3 presents the passivity and structure-preserving discretization of the 2-D vibro-acoustic system with a specific choice of the basis functions and furthermore, the control oriented explicit finite dimensional port-Hamiltonian system is derived. In Section 4, an energy based control is designed using the discretized model using the energy-Casimir method. The numerical simulation results are shown in Section 5 to illustrate the effectiveness of the proposed discretization scheme and passive controller. At last, we conclude this paper by Section 6 and then give some interest perspectives.

2. Port-Hamiltonian formulation of a 2-D vibro-acoustic tube

2.1 *Infinite dimensional port-Hamiltonian system*

The infinite dimensional port-Hamiltonian representation for the system of two conservation laws with canonical interdomain coupling, written in terms of exterior differential calculus on a n-dimensional spatial domain $\mathscr{Z}$ can be decomposed in *structure*, *dynamics* and *constitutive equation* [van der Schaft and Maschke, 2002].

$$\begin{bmatrix} f^p \\ f^q \end{bmatrix} = \begin{bmatrix} 0 & (-1)^r \mathrm{d} \\ \mathrm{d} & 0 \end{bmatrix} \begin{bmatrix} e^p \\ e^q \end{bmatrix} \qquad \text{Structure} \tag{1}$$

$$\begin{bmatrix} f^p \\ f^q \end{bmatrix} = \begin{bmatrix} -\frac{\partial \alpha^p}{\partial t} \\ -\frac{\partial \alpha^q}{\partial t} \end{bmatrix} \qquad \text{Dynamics} \tag{2}$$

$$\begin{bmatrix} e^p \\ e^q \end{bmatrix} = \begin{bmatrix} \delta_{\alpha^p} H \\ \delta_{\alpha^q} H \end{bmatrix} \qquad \text{Constitutive Equations.} \tag{3}$$

The state space X is defined as $X := \Omega^{n_p}(\mathscr{Z}) \times \Omega^{n_q}(\mathscr{Z})$ with $n_p + n_q = n+1$, $r = n_p n_q + 1$ and Ω^{n_p} is the space of n_p forms. An element of the space X is denoted by $x = \begin{bmatrix} \alpha^p & \alpha^q \end{bmatrix}^T$ with state variables

$\alpha^p \in \Omega^{n_p}(\mathscr{Z})$ and $\alpha^q \in \Omega^{n_q}(\mathscr{Z})$. The flow variables $f^p = -\partial_t \alpha^p \in \Omega^{n_p}(\mathscr{Z})$[1] and $f^q = -\partial_t \alpha^q \in \Omega^{n_q}(\mathscr{Z})$ define the vector of flows $f = \begin{bmatrix} f^p & f^q \end{bmatrix}^T \in \mathscr{F} := \Omega^{n_p}(\mathscr{Z}) \times \Omega^{n_q}(\mathscr{Z})$. The effort variable $e^p = \delta_{\alpha^p} H \in \Omega^{n-n_p}(\mathscr{Z})$ and $e^q = \delta_{\alpha^q} H \in \Omega^{n-n_q}(\mathscr{Z})$ define the vector of efforts $e = \begin{bmatrix} e^p & e^q \end{bmatrix}^T \in \mathscr{E} := \Omega^{n-n_p}(\mathscr{Z}) \times \Omega^{n-n_q}(\mathscr{Z})$. Flows and efforts represent dual, power-conjugated variables. The exterior derivative $\mathrm{d} : \Omega^{n-1}(\mathscr{Z}) \mapsto \Omega^n(\mathscr{Z})$ represents the different differential operators from vector calculus. $\delta_{\alpha^p} H$ and $\delta_{\alpha^q} H$ are the variational derivatives of the *energy* or *Hamiltonian functional* $H = \int_{\mathscr{Z}} \mathscr{H}$ with the Hamiltonian density $\mathscr{H} : \Omega^{n_p}(\mathscr{Z}) \times \Omega^{n_q}(\mathscr{Z}) \times \mathscr{Z} \mapsto \Omega^n(\mathscr{Z})$. The boundary variables of the PH formulation (1) are defined by

$$\begin{bmatrix} f^B \\ e^B \end{bmatrix} = \begin{bmatrix} 1 & 0 \\ 0 & -(-1)^{n-n_q} \end{bmatrix} \begin{bmatrix} e^p|_{\partial\mathscr{Z}} \\ e^q|_{\partial\mathscr{Z}} \end{bmatrix} \qquad \text{Boundary Variable} \tag{4}$$

with $\partial\mathscr{Z}$ the $n-1$ dimensional boundary of the spatial domain $\mathscr{Z}$. The space of all admissible flows and efforts satisfying (1), (4) represents a Stokes-Dirac structure [van der Schaft and Maschke, 2002], with respect to the natural pairing

$$\int_{\mathscr{Z}} e^q \wedge f^q + \int_{\mathscr{Z}} e^p \wedge f^p + \int_{\partial\mathscr{Z}} e^B \wedge f^B. \tag{5}$$

2.2 *The 2D vibro-acoustic tube description and its port-Hamiltonian formulation*

We consider a cylindrical tube as in [David et al., 2010], in which an acoustic wave evolves without energy loss as shown in Fig. 1. The source of the acoustic wave is the pressure produced by a loudspeaker on the left side of the tube. An anechoic chamber avoids reflections of the wave at the other side of the tube. The control surface is composed of a set of microphone-loudspeakers that are used to attenuate the wave propagation. The control or attenuation of the acoustic wave is carried out through the motion of the membrane of the loudspeakers which act on the velocity of the wave at the boundary of the acoustic domain. The measurement is the pressure at the right side of the tube.

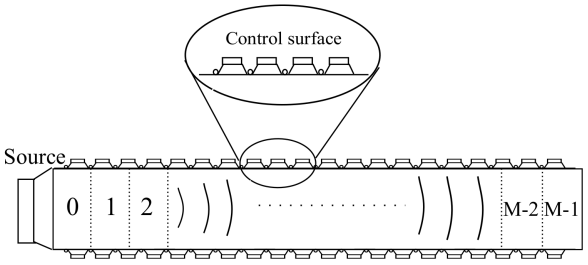

FIG. 1. Cylindrical vibro-acoustic tube and its control component

We first consider an axial symmetry for this system as in Fig. 2 [Trang Vu et al., 2019, Wu et al., 2015]. This allows to reduce the system from 3D coordinates (x, y, ϕ) to 2D coordinates (x, r) where $x \in [0, L]$, $r \in [0, R]$, L, R are the length and radius of the tube respectively, in a power preserving way by a simple change of variables (explicited later).

[1] Denote the operator $\frac{\partial}{\partial t}$ by ∂_t and $\frac{\partial}{\partial x}$ by ∂_x for the sake of simplification.

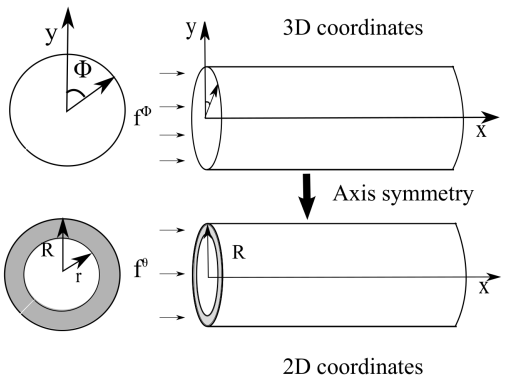

FIG. 2. Reduction from 3D to 2D model by axisymmetry

The 2D infinite dimensional vibro-acoustic system is written as port-Hamiltonian system: $\mathscr{Z}$ is a 2-dimensional smooth manifold with 1-dimensional smooth boundary $\partial\mathscr{Z}$, *i.e.* $n=2$. The state space X is defined as $X := \Omega^2(\mathscr{Z}) \times \Omega^1(\mathscr{Z})$ with $n_p = 2$ and $n_q = 1$. The state vector, element of X is denoted by $x = [\theta, \Gamma]^T$ with θ the kinetic momentum (1-form) , and Γ the volumetric expansion (2-form). The spaces $\mathscr{F}, \mathscr{E}$ are defined as $\mathscr{F} := \Omega^2(\mathscr{Z}) \times \Omega^1(\mathscr{Z})$, and $\mathscr{E} := \Omega^0(\mathscr{Z}) \times \Omega^1(\mathscr{Z})$. The elements $f^x \in \mathscr{F}$, $e^x \in \mathscr{E}$ are given as $f^x = -[\dot{\theta}, \dot{\Gamma}]^T$ and $e^x = [v, P]^T$ where v is the velocity (1-form) and P is the pressure (0-form). The flow variable f^θ (1-form) of the 2D model is obtained by flow f^Φ (2-form) of the 3D model with $f^\theta = 2\pi r f^\Phi$ as in Figure 2. This means the 2D variable f^θ is the projection of the flow variable f^Φ over a circle of given radius from a point based on the axial symmetry.

The *total energy* is given by:

$$H = \frac{1}{2}\int_{\mathscr{Z}} \theta \wedge \frac{*\theta}{\rho_0} + \Gamma \wedge \frac{*\Gamma}{\chi_s} \tag{6}$$

with $*$ the Hodge star operator which converts any k-form w on a n-dimensional spatial domain $\mathscr{Z}$ to an $(n-k)$-form $*w$. Here ρ_0 is the air mass density, χ_s is the adiabatic compressibility coefficient.

The port-Hamiltonian representation of the vibro-acoustic system defined on a 2D spatial domain[2] $\mathscr{Z} := (x,y) = z \subset \mathbb{R}^2$ is:

$$\begin{bmatrix} f^\theta \\ f^\Gamma \end{bmatrix} = \begin{bmatrix} 0 & -\mathrm{d} \\ \mathrm{d} & 0 \end{bmatrix} \begin{bmatrix} e^v \\ e^p \end{bmatrix} \quad \text{Structure} \tag{7}$$

$$\begin{bmatrix} f^\theta \\ f^\Gamma \end{bmatrix} = \begin{bmatrix} -\dot{\theta} \\ -\dot{\Gamma} \end{bmatrix} \quad \text{Dynamics} \tag{8}$$

$$\begin{bmatrix} e^v \\ e^p \end{bmatrix} = \begin{bmatrix} \delta_\theta H \\ \delta_\Gamma H \end{bmatrix} \quad \text{Constitutive Equations, } H \text{ being defined by (6)} \tag{9}$$

$$\begin{bmatrix} f^B \\ e^B \end{bmatrix} = \begin{bmatrix} 1 & 0 \\ 0 & 1 \end{bmatrix} \begin{bmatrix} e^v|_{\partial\mathscr{Z}} \\ e^p|_{\partial\mathscr{Z}} \end{bmatrix} \quad \text{Boundary Variables} \tag{10}$$

[2]Since the 2D system of coordinates is now rectangular, we use (x,y) instead of (x,r) to denote the spatial domain.

3. Discretization of the 2D vibro-acoustic system

In this section, we propose a structure-preserving mixed finite elements discretization method, to derive a finite dimensional approximation of (7) and (10).

3.1 *Approximation of the Dirac structure*

Taking the spatial domain geometry of the system into account, we use square grid elements instead of triangular ones found in the literature [Golo et al., 2004]. The square grid element $\mathscr{Z}_{abcd}$ is defined by four vertices a, b, c, d. The edges of the square are defined by ab, bc, cd, da and the facet by $abcd$.

We approximate the flow and effort variables on the square grids by using the space dependent basis forms. The objective is to separate flow and effort variables $f(t,z)$ and $e(t,z)$ to only time dependent flow and effort approximations in the grid $f_{\mathscr{Z}_{abcd}}(t)$, $e_{\mathscr{Z}_{abcd}}(t)$ and the space basis function $w_{\mathscr{Z}_{abcd}}(z)$. For the sake of simplification, we omit (t) and (z) for the approximated variables and basis functions respectively.

The flow variables defined in (8) are approximated by:

$$f^{\theta}(t,z) = f^{\theta}_{ab}w^{\theta}_{ab} + f^{\theta}_{bc}w^{\theta}_{bc} + f^{\theta}_{cd}w^{\theta}_{cd} + f^{\theta}_{da}w^{\theta}_{da} \tag{11}$$

$$f^{\Gamma}(t,z) = f^{\Gamma}_{abcd}w^{\Gamma}_{abcd} \tag{12}$$

where the 1-forms w^{θ}_{l}, $l \in \{ab, bc, cd, da\}$, and the 2-form w^{Γ}_{abcd} satisfy the following conditions[3]

$$\int_{l'} w^{\theta}_{l} = \begin{cases} 0 \, if \, l' \neq l, \\ 1 \, if \, l' = l, \end{cases} \qquad \int_{\mathscr{Z}_{abcd}} w^{\Gamma}_{abcd} = 1 \tag{13}$$

The effort variables defined in (9), the velocity (1-form) e^{v} and the pressure (0-form) e^{p}, are approximated by:

$$e^{v}(t,z) = e^{v}_{ab}w^{v}_{ab} + e^{v}_{bc}w^{v}_{bc} + e^{v}_{cd}w^{v}_{cd} + e^{v}_{da}w^{v}_{da} \tag{14}$$

$$e^{p}(t,z) = e^{p}_{a}w^{p}_{a} + e^{p}_{b}w^{p}_{b} + e^{p}_{c}w^{p}_{c} + e^{p}_{d}w^{p}_{d} \tag{15}$$

where the one-forms w^{v}_{l}, $l \in \{ab, bc, cd, da\}$, and the zero-form w^{p}_{m}, $m \in \{a, b, c, d\}$, satisfy the following conditions[4]:

$$\int_{l'} w^{v}_{l} = \begin{cases} 0 & if \, l' \neq l, \\ 1 & if \, l' = l, \end{cases} \quad w^{p}_{m'}(m) = \begin{cases} 0 & m' \neq m \\ 1 & m' = m \end{cases} \tag{16}$$

The structure of the vibro-acoustic system (7) can be approximated by substituting the flows approximations (11), (12) and the efforts approximations (14), (15) into (7):

$$f^{\theta}_{ab}w^{\theta}_{ab} + f^{\theta}_{bc}w^{\theta}_{bc} + f^{\theta}_{cd}w^{\theta}_{cd} + f^{\theta}_{da}w^{\theta}_{da} = \text{-d}\left(e^{p}_{a}w^{p}_{a} + e^{p}_{b}w^{p}_{b} + e^{p}_{c}w^{p}_{c} + e^{p}_{d}w^{p}_{d}\right) \tag{17}$$

$$f^{\Gamma}_{abcd}w^{\Gamma}_{abcd} = \text{d}(e^{v}_{ab}w^{v}_{ab} + e^{v}_{bc}w^{v}_{bc} + e^{v}_{cd}w^{v}_{cd} + e^{v}_{da}w^{v}_{da}) \tag{18}$$

In order to satisfy (17) and (18), we deduce the compatibility conditions between the two forms and one forms, and between the one forms and the zero-forms [Golo et al., 2004]. Supposing $e^{p}_{b} = e^{p}_{c} =$

[3]These condition state that the flow variable $f^{\Gamma}(t,z)$ coincides with f^{Γ} on the rectangular surface $abcd$ and $f^{\theta}(t,z)$ coincides with f^{θ}_{l} on the edge $l \in \{ab, bc, cd, cd\}$.

[4]These condition state thatthat the effort variable pressure $e^{p}(t,z)$ coincides with e^{p} on the node $m \in \{a, b, c, d\}$ and the velocity $e^{v}(t,z)$ coincides with e^{v} on the edge $l \in ab, bc, cd, cd$.

$e_d^p = 0$, (17) is satisfied if and only if $dw_a^p(z) = \gamma_{ab} w_{ab}^\theta(z) + \gamma_{bc} w_{bc}^\theta(z) + \gamma_{cd} w_{cd}^\theta(z) + \gamma_{da} w_{da}^\theta(z)$. Thus, $\int_{ab} dw_a^p(z) = \int_{ab} (\gamma_{ab} w_{ab}^\theta(z) + \gamma_{bc} w_{bc}^\theta(z) + \gamma_{cd} w_{cd}^\theta(z) + \gamma_{da} w_{da}^\theta(z))$. Integrating along ab, bc,cd and da gives $\gamma_{ab} = -1$, $\gamma_{bc} = 0$, $\gamma_{cd} = 0$ and $\gamma_{da} = 1$. Similarly, we get the following conditions:

$$\begin{array}{rclrcl} dw_a^p &=& w_{da}^\theta - w_{ab}^\theta; & dw_b^p &=& w_{ab}^\theta - w_{bc}^\theta; \\ dw_c^p &=& w_{dc}^\theta - w_{cd}^\theta; & dw_d^p &=& w_{cd}^\theta - w_{da}^\theta;; \\ dw_i^y &=& w_{abcd}^\Gamma & i &\in& \{ab, bc, cd, da\}. \end{array} \tag{19}$$

The finite dimensional Dirac structure of the square grid (Fig. 3) can be find in the Appendix 1. To write the dynamic equation of the 2D vibro-acoustic system with finite dimensional Dirac structure, we have to define the basis functions w_{abcd}, w_l with $l \in \{ab, bc, cd, da\}$ and w_m with $m \in \{a, b, c, d\}$ such that the parameters α, β and γ of the Dirac structure are explicit. In order to get an explicit system, in [Wu et al., 2015], simplified parameters α, β and γ which do not satisfy the basis function conditions (13), (16) and the compatibility conditions (19) are used. In this paper, we will select these parameters such that these conditions are satisfied.

Consider the square grid shown in Fig. 3. The position of every vertices is defined as $a : (x_1, y_1)$, $b : (x_2, y_1)$, $c : (x_2, y_2)$ and $d : (x_1, y_2)$. Consider as two forms weight function:

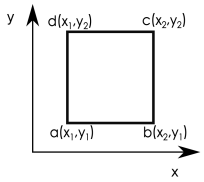

FIG. 3. An discretized square grid

$$w_{abcd} = \frac{1}{(x_2 - x_1)(y_2 - y_1)} dx \wedge dy \tag{20}$$

which satisfies (13). The one-form basis functions w_l with $l \in \{ab, bc, cd, da\}$ and the zero-form basis functions w_m with $m \in \{a, b, c, d\}$ are defined as

$$\begin{array}{ll} w_{ab} = \frac{(y_2 - y)}{(x_2 - x_1)(y_2 - y_1)} dx; & w_{bc} = \frac{(x - x_1)}{(x_2 - x_1)(y_2 - y_1)} dy; \\ w_{cd} = \frac{(y_1 - y)}{(x_2 - x_1)(y_2 - y_1)} dx & w_{da} = \frac{(x - x_2)}{(x_2 - x_1)(y_2 - y_1)} dy. \end{array} \tag{21}$$

$$\begin{array}{ll} w_a = \frac{(x_2 - x)}{(x_2 - x_1)} \frac{(y_2 - y)}{(y_2 - y_1)}; & w_b = \frac{(x - x_1)}{(x_2 - x_1)} \frac{(y_2 - y)}{(y_2 - y_1)}; \\ w_c = \frac{(x - x_1)}{(x_2 - x_1)} \frac{(y - y_1)}{(y_2 - y_1)}; & w_d = \frac{(x_2 - x)}{(x_2 - x_1)} \frac{(y - y_1)}{(y_2 - y_1)}, \end{array} \tag{22}$$

and satisfy (16). After some computation, one can check the compatibility conditions (19) are satisfied.

With the above basis functions, one can write the finite dimensional Dirac structure of a square grid

as follow:

$$\begin{bmatrix} \frac{1}{4} & 0 & 0 & 0 & \frac{1}{2} & 0 & 0 & \frac{1}{2} \\ \frac{1}{4} & 0 & 0 & 0 & \frac{1}{2} & \frac{1}{2} & 0 & 0 \\ \frac{1}{4} & 0 & 0 & 0 & 0 & \frac{1}{2} & \frac{1}{2} & 0 \\ \frac{1}{4} & 0 & 0 & 0 & 0 & 0 & \frac{1}{2} & \frac{1}{2} \\ 0 & -\frac{1}{4} & -\frac{1}{4} & -\frac{1}{2} & 0 & 0 & 0 & 0 \\ 0 & -\frac{1}{4} & \frac{1}{4} & 0 & 0 & 0 & 0 & 0 \\ 0 & \frac{1}{4} & \frac{1}{4} & \frac{1}{2} & 0 & 0 & 0 & 0 \\ 0 & \frac{1}{4} & -\frac{1}{4} & 0 & 0 & 0 & 0 & 0 \end{bmatrix} \begin{bmatrix} f^{\Gamma}_{abcd} \\ f^{\theta}_{ab} \\ f^{\theta}_{cd} \\ f^{\theta}_{da} \\ f^{B}_{ab} \\ f^{B}_{bc} \\ f^{B}_{cd} \\ f^{B}_{da} \end{bmatrix} + \begin{bmatrix} 0 & 1 & 0 & -1 & 0 & 0 & 0 & 0 \\ 0 & -1 & 0 & 0 & 0 & 0 & 0 & 0 \\ 0 & 0 & 1 & 0 & 0 & 0 & 0 & 0 \\ 0 & 0 & -1 & 1 & 0 & 0 & 0 & 0 \\ 1 & 0 & 0 & 0 & 1 & 0 & 0 & 0 \\ 1 & 0 & 0 & 0 & 0 & 1 & 0 & 0 \\ 1 & 0 & 0 & 0 & 0 & 0 & 1 & 0 \\ 1 & 0 & 0 & 0 & 0 & 0 & 0 & 1 \end{bmatrix} \begin{bmatrix} e^{\Gamma}_{abcd} \\ e^{\theta}_{ab} \\ e^{\theta}_{cd} \\ e^{\theta}_{da} \\ e^{B}_{ab} \\ -e^{B}_{bc} \\ -e^{B}_{cd} \\ e^{B}_{da} \end{bmatrix} = 0. \tag{23}$$

The variables f^B_l and e^B_l with $l \in \{ab, bc, cd, da\}$ stand for the boundary velocities and pressure at the boundary (four edges $\{ab, bc, cd, da\}$) of the discretized square grid. The variable f^{Γ}_{abcd} is the approximation of the variable f^{Γ} over the square grid $abcd$. The variable e^{Γ}_{abcd} is the power conjugate variable of f^{Γ}_{abcd} which is obtained by the approximation of the zero form variables e^p_m ($m \in \{a, b, c, d\}$) such that the potential power over the square grid is $\int_{\mathscr{Z}} e^p(t,z) \wedge f^{\Gamma}(t,z) = f^{\Gamma}_{abcd} \wedge e^{\Gamma}_{abcd}$. From the power preserving point of view, the port variables $(f^{\theta}_{ab}, e^{\theta}_{ab})$, $(f^{\theta}_{cd}, e^{\theta}_{cd})$, $(f^{\theta}_{da}, e^{\theta}_{da})$ are defined from the approximation of the discretized one form variables f^{θ}_l and e^v_l with $l \in \{ab, bc, cd, da\}$such that the kinetic power over the discretized square grid are $\int_{\mathscr{Z}} e^v(t,z) \wedge f^{\theta}(t,z) = f^{\theta}_{ab} e^{\theta}_{ab} + f^{\theta}_{cd} e^{\theta}_{cd} + f^{\theta}_{da} e^{\theta}_{da}$. Please find more details in Appendix 1.

3.2 *Discretization of 2D vibro-acoustic system*

In the previous subsection, we discussed the approximation of the Dirac structure over a square grid. In this section, we derive from this elementary model the explicit port-Hamiltonian formulation of the 2-D vibro-acoustic tube. To this end, we consider that the over all 2D vibro-acoustic tube is discretized in $N \times M$ elements with N rows overn the vertical direction and M rows over the horizontal direction. The interconnection is proceeded in two steps as shown in Fig. 4. First, the N elements (0 to $N-1$) are vertically interconnected and then all the M vertical elements are interconnected horizontally (like element j to $j+1$ with $j \in \{0, 1, \cdots, M-1\}$) as shown in Fig. 4. We present the explicit input-output representation of each square and then the complete system with the vertical and horizontal interconnections.

3.3 *Explicit input-output representation by interconnection*

The first step consists in interconnecting vertically the element 0 to $N-1$ of each single column. However, we have to notice that the boundary conditions of the bottom element 0 is different from the ones of elements 1 to $N-1$. That is because the physical input of the vibro-acoustic tube is the pressure on the left side and the control variables on the top boundary of the tube is the velocity due to the control membrane interconnected to the tube. The output measurement of the tube is the pressure on the right side. From the above input-output consideration, the inputs of each element are the pressure on the left and bottom sides and the velocity on the right and top sides. However, from the axis symmetry assumption, the boundary condition on the bottom of the tube is the velocity $v = 0$ which should be considered as the input. This boundary condition and the input-output consideration present a causality contradiction. In order to deal with this causality, a different input-output configuration shall be considered on element 0.

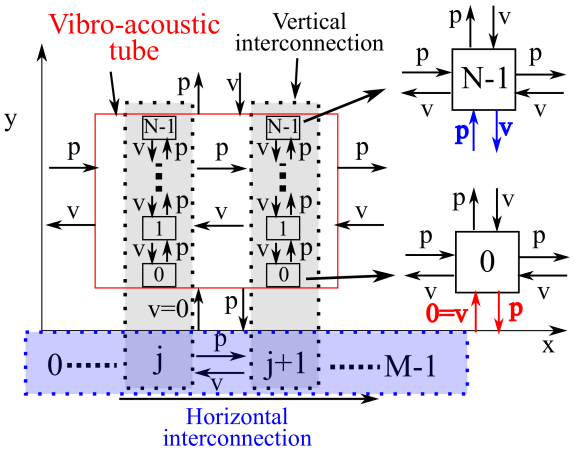

FIG. 4. Interconnection relation of vibro-acoustic tube

With the above boundary conditions, we first consider the inputs and outputs of the explicit representation for the square grid of elements 1 to $N-1$ as follows:

$$\begin{bmatrix} u_1 \\ u_2 \\ u_3 \\ u_4 \end{bmatrix} = \begin{bmatrix} e^B_{ab} \\ f^B_{bc} \\ f^B_{cd} \\ e^B_{da} \end{bmatrix} = \begin{bmatrix} p_{ab} \\ v_{bc} \\ v_{cd} \\ p_{da} \end{bmatrix}, \quad \begin{bmatrix} y_1 \\ y_2 \\ y_3 \\ y_4 \end{bmatrix} = \begin{bmatrix} f^B_{ab} \\ -e^B_{bc} \\ -e^B_{cd} \\ f^B_{da} \end{bmatrix} = \begin{bmatrix} v_{ab} \\ p_{bc} \\ p_{cd} \\ v_{da} \end{bmatrix}. \tag{24}$$

Taking into account the above input-output variables and the Dirac structure of the square grid (23) with the following dynamics:

$$\begin{bmatrix} -\dot{x}_1 \\ -\dot{x}_2 \\ -\dot{x}_3 \\ -\dot{x}_4 \end{bmatrix} = \begin{bmatrix} f_1 \\ f_2 \\ f_3 \\ f_4 \end{bmatrix} = \begin{bmatrix} f^\Gamma_{abcd} \\ f^\theta_{ab} \\ f^\theta_{cd} \\ f^\theta_{da} \end{bmatrix}, \quad \begin{bmatrix} e_1 \\ e_2 \\ e_3 \\ e_4 \end{bmatrix} = \begin{bmatrix} e^\Gamma_{abcd} \\ e^\theta_{ab} \\ e^\theta_{cd} \\ e^\theta_{da} \end{bmatrix}, \tag{25}$$

with the energy variables $x = [x_1, x_2, x_3, x_4]^T$, the explicit port-Hamiltonian representation for the elements 1 to $N-1$ can be written as:

$$\begin{cases} \begin{bmatrix} \dot{x}_1 \\ \dot{x}_2 \\ \dot{x}_4 \end{bmatrix} = \begin{bmatrix} 0 & -4 & 4 \\ 4 & 0 & 0 \\ -4 & 0 & 0 \end{bmatrix} \begin{bmatrix} e_1 \\ e_2 \\ e_4 \end{bmatrix} + \begin{bmatrix} 0 & 2 & 2 & 0 \\ -4 & 0 & 0 & 0 \\ 2 & 0 & 0 & 2 \end{bmatrix} \begin{bmatrix} u_1 \\ u_2 \\ u_3 \\ u_4 \end{bmatrix} \\ \begin{bmatrix} y_1 \\ y_2 \\ y_3 \\ y_4 \end{bmatrix} = \begin{bmatrix} 0 & -4 & 2 \\ 2 & 0 & 0 \\ 2 & 0 & 0 \\ 0 & 0 & 2 \end{bmatrix} \begin{bmatrix} e_1 \\ e_2 \\ e_4 \end{bmatrix} + \begin{bmatrix} 0 & 0 & -1 & 0 \\ 0 & 0 & 0 & 1 \\ 1 & 0 & 0 & 0 \\ 0 & -1 & 0 & 0 \end{bmatrix} \begin{bmatrix} u_1 \\ u_2 \\ u_3 \\ u_4 \end{bmatrix} \end{cases} \tag{26}$$

One can notice that the above system does not have dynamic equations in $\dot{x}_3$ and e_3. This is because e_2, e_3 and e_4 are projected velocity variables chosen in order to get a finite dimensional Dirac structure . This choice of variables leads to a singular system with Differential Algebraic equations (DAE) . Hence, in order to avoid the DAE representation of the explicit system, we omit the variable e_3. The variables e_2 and e_4 can be seen as the velocity variables on the horizontal direction x and the vertical direction y, respectively. The constitutive relations (See the details of the computation in the Appendix 2) are:

$$\begin{bmatrix} e_1 \\ e_2 \\ e_4 \end{bmatrix} = \underbrace{\begin{bmatrix} S_{in}\frac{1}{\chi_s} & 0 & 0 \\ 0 & \frac{1}{3}S_{2in}\frac{1}{\rho_0} & -S_{1in}\frac{1}{6\rho_0} \\ 0 & -S_{1in}\frac{1}{6\rho_0} & S_{1in}\frac{1}{\rho_0} \end{bmatrix}}_{Q} \begin{bmatrix} x_1 \\ x_2 \\ x_4 \end{bmatrix} \tag{27}$$

The Hamiltonian function of each element is defined as $H = \frac{1}{2}x^T Qx$. For the purpose of simplicity, we take the notation $\begin{bmatrix} x_1 & x_2 & x_3 \end{bmatrix}^T$ and $\begin{bmatrix} e_1 & e_2 & e_3 \end{bmatrix}^T$ instead of $\begin{bmatrix} x_1 & x_2 & x_4 \end{bmatrix}^T$ and $\begin{bmatrix} e_1 & e_2 & e_4 \end{bmatrix}^T$.

Now we consider the explicit representation of the bottom system 0 from the kernel representation of the Dirac structure (23) with the following choice of inputs and outputs:

$$\begin{bmatrix} u_1 \\ u_2 \\ u_3 \\ u_4 \end{bmatrix} = \begin{bmatrix} f^B_{ab} \\ f^B_{bc} \\ f^B_{cd} \\ e^B_{da} \end{bmatrix} = \begin{bmatrix} v_{ab} \\ v_{bc} \\ v_{cd} \\ p_{da} \end{bmatrix}, \quad \begin{bmatrix} y_1 \\ y_2 \\ y_3 \\ y_4 \end{bmatrix} = \begin{bmatrix} e^B_{ab} \\ -e^B_{bc} \\ -e^B_{cd} \\ f^B_{da} \end{bmatrix} = \begin{bmatrix} p_{ab} \\ p_{bc} \\ p_{cd} \\ v_{da} \end{bmatrix} \tag{28}$$

One can notice that the difference in inputs and outputs between the bottom element and the other elements are u_1 and y_1. In the same manner, the explicit formulation for the element 0 is given by:

$$\begin{cases} \begin{bmatrix} \dot{x}_1 \\ \dot{x}_2 \\ \dot{x}_3 \end{bmatrix} = \begin{bmatrix} 0 & -4 & 4 \\ 4 & 0 & 0 \\ -4 & 0 & 0 \end{bmatrix} \begin{bmatrix} e_1 \\ e_2 \\ e_3 \end{bmatrix} + \begin{bmatrix} 2 & 2 & 2 & 0 \\ 0 & 0 & 0 & -4 \\ 0 & 0 & 0 & 1 \end{bmatrix} \begin{bmatrix} u_1 \\ u_2 \\ u_3 \\ u_4 \end{bmatrix} \\ \begin{bmatrix} y_1 \\ y_2 \\ y_3 \\ y_4 \end{bmatrix} = \begin{bmatrix} 2 & 0 & 0 \\ 2 & 0 & 0 \\ 2 & 0 & 0 \\ 0 & -4 & 1 \end{bmatrix} \begin{bmatrix} e_1 \\ e_2 \\ e_3 \end{bmatrix} + \begin{bmatrix} 0 & 0 & 0 & 0 \\ 0 & 0 & 0 & 1 \\ 0 & 0 & 0 & 0 \\ 0 & -1 & 0 & 0 \end{bmatrix} \begin{bmatrix} u_1 \\ u_2 \\ u_3 \\ u_4 \end{bmatrix} \end{cases} \tag{29}$$

In order to get *vertical interconnection* of all elements, the following interconnection relation is considered:

$$\begin{array}{rcl} u^i_3 & = & y^{i+1}_1 \\ u^{i+1}_1 & = & -y^i_3 \end{array} \quad \text{with} \quad i = 0, \ldots, N-2. \tag{30}$$

Thus the *vertically interconnected* explicit system:

$$\begin{cases} \begin{bmatrix} \dot{\mathbf{x}}_1 \\ \dot{\mathbf{x}}_2 \\ \dot{\mathbf{x}}_3 \end{bmatrix} = \begin{bmatrix} 0 & T_N^1 & T_N^2 \\ -T_N^{1T} & 0 & 0 \\ -T_N^{2T} & 0 & 0 \end{bmatrix} \begin{bmatrix} \mathbf{e}_1 \\ \mathbf{e}_2 \\ \mathbf{e}_3 \end{bmatrix} + \begin{bmatrix} B_N^1 & B_N^2 & B_N^3 & 0 \\ 0 & 0 & 0 & T_N^1 \\ 0 & 0 & 0 & B_N^2 \end{bmatrix} \begin{bmatrix} u_1 \\ \mathbf{u}_2 \\ u_3 \\ \mathbf{u}_4 \end{bmatrix} \\ \begin{bmatrix} y_1 \\ \mathbf{y}_2 \\ y_3 \\ \mathbf{y}_4 \end{bmatrix} = \begin{bmatrix} B_N^{1T} & 0 & 0 \\ B_N^{2T} & 0 & 0 \\ B_N^{3T} & 0 & 0 \\ 0 & T_N^{1T} & B_N^{2T} \end{bmatrix} \begin{bmatrix} \mathbf{e}_1 \\ \mathbf{e}_2 \\ \mathbf{e}_3 \end{bmatrix} + \begin{bmatrix} 0 & 0 & D_1 & 0 \\ 0 & 0 & 0 & I_N \\ -D_1^T & 0 & 0 & 0 \\ 0 & -I_N & 0 & 0 \end{bmatrix} \begin{bmatrix} u_1 \\ \mathbf{u}_2 \\ u_3 \\ \mathbf{u}_4 \end{bmatrix} \end{cases} \tag{31}$$

where 0 represents zero matrices of appropriate dimension and the state variables are $\mathbf{x}_i = \left[x_i^1, x_i^2, \ldots, x_i^{N-1}\right]^T$ with $i \in \{1,2,3\}$. The matrices are defined as

$$T_N^1 = \text{diag}\,[4,4,\cdots,4] \in \mathbb{R}^{N\times N}, \tag{32}$$

$$T_N^2 = \begin{bmatrix} -4 & 0 & 0 & \cdots & 0 \\ 4 & -4 & 0 & \ddots & \vdots \\ -4 & 4 & -4 & \ddots & 0 \\ \vdots & \ddots & \ddots & \ddots & 0 \\ (-1)^N 4 & \cdots & -4 & 4 & -4 \end{bmatrix} \in \mathbb{R}^{N\times N} \tag{33}$$

$$B_N^1 = \begin{bmatrix} -2 \\ 2 \\ \vdots \\ (-1)^N 2 \end{bmatrix}, B_N^2 = \text{diag}\,[-2,-2,\cdots,-2] \in \mathbb{R}^{N\times N}, \tag{34}$$

$$B_N^3 = \begin{bmatrix} (-1)^{N-1} 2 \\ \vdots \\ -2 \\ 2 \end{bmatrix}, D_1 = \begin{bmatrix} -1 \\ 0 \\ \vdots \\ 0 \end{bmatrix} \in \mathbb{R}^N. \tag{35}$$

The inputs and outputs of each vertically interconnected explicit system are defined as follows: the pressure inputs and velocity outputs at the left side and the top of the tube, the velocity inputs and the pressure measurement at the right side and the bottom of the tube,

$$u_1 = u_1^0 = v_{ab}^0; y_1 = y_1^0 = p_{ab}^0; \tag{36}$$

$$\mathbf{u}_2 = \begin{bmatrix} v_{bc}^0 \\ v_{bc}^1 \\ \vdots \\ v_{bc}^{N-1} \end{bmatrix}; \mathbf{y}_2 = \begin{bmatrix} p_{bc}^0 \\ p_{bc}^1 \\ \vdots \\ p_{bc}^{N-1} \end{bmatrix}; \tag{37}$$

$$u_3 = u_3^{N-1} = v_{cd}^{N-1}; y_3 = y_3^{N-1} = p_{cd}^{N-1}; \tag{38}$$

The left side of each vertically interconnected system has the pressure as input which corresponds to the physical input and its power conjugate output is the corresponding velocity:

$$\mathbf{u}_4 = \begin{bmatrix} p_{da}^0 \\ p_{da}^1 \\ \vdots \\ p_{da}^{N-1} \end{bmatrix}; \mathbf{y}_4 = \begin{bmatrix} v_{da}^0 \\ v_{da}^1 \\ \vdots \\ v_{da}^{N-1} \end{bmatrix}. \tag{39}$$

Now we discuss the horizontal interconnection of each obtained vertical element (31). The input on the left side of each vertical element is the pressure while it is the output on the right side. Thus, the interconnection relation between each vertical element (31) is given as:

$$\begin{array}{rcl} \mathbf{u}_2^j & = & \mathbf{y}_4^{j+1} \\ \mathbf{u}_4^{j+1} & = & -\mathbf{y}_2^j \end{array} \quad \text{with} \quad j = 0, \ldots, M-2. \tag{40}$$

With the above relations, we obtain the interconnected system:

$$\begin{cases} \begin{bmatrix} \dot{\tilde{\mathbf{x}}}_1 \\ \dot{\tilde{\mathbf{x}}}_2 \\ \dot{\tilde{\mathbf{x}}}_3 \end{bmatrix} = \mathbf{J} \begin{bmatrix} \tilde{\mathbf{e}}_1 \\ \tilde{\mathbf{e}}_2 \\ \tilde{\mathbf{e}}_3 \end{bmatrix} + \mathbf{B} \begin{bmatrix} \mathbf{u}_1 \\ \mathbf{u}_2 \\ \mathbf{u}_3 \\ \mathbf{u}_4 \end{bmatrix} \\ \begin{bmatrix} \mathbf{y}_1 \\ \mathbf{y}_2 \\ \mathbf{y}_3 \\ \mathbf{y}_4 \end{bmatrix} = \mathbf{B}^T \begin{bmatrix} \tilde{\mathbf{e}}_1 \\ \tilde{\mathbf{e}}_2 \\ \tilde{\mathbf{e}}_3 \end{bmatrix} + \mathbf{D} \begin{bmatrix} \mathbf{u}_1 \\ \mathbf{u}_2 \\ \mathbf{u}_3 \\ \mathbf{u}_4 \end{bmatrix} \end{cases} \tag{41}$$

where the state variable are $\tilde{\mathbf{x}}_i = \left[\mathbf{x}_i^0, \mathbf{x}^1, \ldots, \mathbf{x}_i^{M-1}\right]^T$ with $i \in \{1,2,3\}$. The constitutive relation of the discretized system can be written as:

$$\tilde{\mathbf{e}} = \begin{bmatrix} S_1 & 0 & 0 \\ 0 & S_2 & S_4 \\ 0 & S_4^T & S_3 \end{bmatrix} \mathbf{x} = \tilde{\mathbf{Q}}\mathbf{x} \tag{42}$$

with $S_1 = \text{diag}\left[S_{in}\frac{1}{\chi_s}\right]$, $S_2 = \text{diag}\left[\frac{1}{3}S_{2in}\frac{1}{\rho_0}\right]$, $S_3 = \text{diag}\left[S_{1in}\frac{1}{\rho_0}\right]$, and $S_4 = \text{diag}\left[-S_{1in}\frac{1}{6\rho_0}\right]$.

The inputs are the velocity at the bottom $\{ab\}$, the right side $\{bc\}$ and the top $\{cd\}$ of the tube, respectively, $\mathbf{u}_1 = \left[v_{ab}^0, v_{ab}^1, \ldots, v_{ab}^{M-1}\right]^T$, $\mathbf{u}_2 = \left[v_{bc}^0, v_{bc}^1, \ldots, v_{bc}^{N-1}\right]^T$, $\mathbf{u}_3 = \left[v_{cd}^0, v_{cd}^1, \ldots, v_{cd}^{M-1}\right]^T$, and the pressure on the right side $\{da\}$ of the tube, $\mathbf{u}_4 = \left[p_{da}^0, p_{da}^1, \ldots, p_{da}^{N-1}\right]^T$. The outputs are the power conjugate variables of the inputs, *i.e.*, the pressure on the top, the bottom and the right side, the velocity on the left side of the vibro-acoustic tube. The interconnection matrix, input matrix and the feedforward matrix are given by:

$$\mathbf{J} = \begin{bmatrix} 0 & \tilde{T}_{1M} & \tilde{T}_{2M} \\ -\tilde{T}_{1M}^T & 0 & 0 \\ -\tilde{T}_{2M}^T & 0 & 0 \end{bmatrix}; \tag{43}$$

$$\mathbf{B} = \begin{bmatrix} \tilde{B}_M^1 & \tilde{B}_M^2 & \tilde{B}_M^3 & 0 \\ 0 & 0 & 0 & T_M^{1B} \\ 0 & 0 & 0 & -\tilde{B}_M^2 \end{bmatrix}; \tag{44}$$

$$\mathbf{D} = \begin{bmatrix} 0 & 0 & 0 & 0 \\ 0 & 0 & 0 & (-1)^{M-1} I_{N\times N} \\ 0 & 0 & 0 & 0 \\ 0 & (-1)^M I_{N\times N} & 0 & 0 \end{bmatrix} \tag{45}$$

with 0 zero matrices of appropriate dimension and the sub-matrices are given by:

$$\tilde{T}_{1M} = \begin{bmatrix} T_{1N} & 0 & \cdots & 0 \\ -B_N^2 T_{1N}^T & T_{1N} & \ddots & \vdots \\ \vdots & \ddots & \ddots & 0 \\ (-1)^{M-1} B_N^2 T_{1N}^T & \cdots & -B_N^2 T_{1N}^T & T_{1N} \end{bmatrix};$$

$$\tilde{T}_{2M} = \begin{bmatrix} T_{2N} & 0 & \cdots & 0 \\ -B_N^2 B_N^{2T} & T_{2N} & \ddots & \vdots \\ \vdots & \ddots & \ddots & 0 \\ (-1)^{M-1} B_N^2 B_N^{2T} & \cdots & -B_N^2 B_N^{2T} & T_{2N} \end{bmatrix};$$

$$T_M^{1B} = \begin{bmatrix} (-1)^{M-1} T_N^1 \\ \vdots \\ -T_N^1 \\ T_N^1 \end{bmatrix}; \; \bar{B}_M^1 = \operatorname{diag}\left[B_N^1\right];$$

$$\tilde{B}_M^2 = \begin{bmatrix} (-1)^{M-1} B_N^2 \\ \vdots \\ -B_N^2 \\ B_N^2 \end{bmatrix}; \; \tilde{B}_M^3 = \operatorname{diag}\left[B_N^3\right].$$

4. Control by interconnection

In this section, we consider a control based on the discretised model (41) by using energy shaping through Casimir invariants. We consider that the vibro-acoustic tube is actuated all over its length by a distributed set of actuators and sensors. In this example we consider a possible large set of actuators/sensors(small enough) in order to consider quasi continuous actuation. From the axis-symmetry assumption, the control surface acts only on the top $\{bc\}$ of the 2D vibro-acoustic system.

The control surface is composed of a set of microphone-loudspeakers that are used to attenuate the wave pressure in the tube or to change the wave properties in a desired manner.

We propose to derive a control law which attenuates the wave pressure controlling the membrane of the loudspeakers. To this end we employ the well known control by interconnection approach, in which the existence of closed-loop invariants are used to design a controller which assigns the closed-loop Hamiltonian function. A detailed survey on this approach can be found in [van der Schaft, 2000].

Consider the following port-Hamiltonian controller:

$$\left\{\begin{array}{rcl} \dot{\xi} & = & (J_c(\xi)-R(\xi))\frac{\partial H_c}{\partial \xi}(\xi)+g_c(\xi)u_c \\ y_c & = & g_c^T(\xi)\frac{\partial H_c}{\partial \xi}(\xi) \end{array}\right. \tag{46}$$

with state variable $\xi \in \mathbb{R}^M$, Hamiltonian function $H_c(\xi)$ and structure matrices $J_c(\xi) = -J_c(\xi)^T$ and $R_c(\xi) = R_c(\xi)^T \geqslant 0$. The controller and the system are interconnected at the top (cd boundary) of the tube with the membrane, i.e. the wave propagation is controlled by the velocity injected by membrane and the pressure of the wave on the same boundary can be seen as the reaction force to the controller. Hence the power preserving interconnection of the controller and the system are:

$$\begin{array}{rcl} \mathbf{u}_3 & = & -y_c \\ u_c & = & \mathbf{y}_3 \end{array} \tag{47}$$

Thus, the coupling system of wave propagation (41) and the controller (46) via the above interconnection law (47) is still passive and can be written as:

$$\begin{bmatrix} \dot{\mathbf{x}} \\ \dot{\xi} \end{bmatrix} = \left(\begin{bmatrix} \mathbf{J} & -\tilde{B}_M^3 g_c^T(\xi) \\ g_c(\xi)\tilde{B}_M^{3T} & J_c(\xi) \end{bmatrix} - \begin{bmatrix} 0 & 0 \\ 0 & R_c(\zeta) \end{bmatrix} \right) \begin{bmatrix} \frac{\partial H_d}{\partial \mathbf{x}}(\mathbf{x}) \\ \frac{\partial H_d}{\partial \xi}(\xi) \end{bmatrix}$$

where $H_d(\tilde{\mathbf{x}}, \xi) = \mathbf{H}(\tilde{\mathbf{x}}) + H_c(\xi)$ is the energy of the closed-loop system with the open loop vibro-acoustic energy $\mathbf{H}(\tilde{\mathbf{x}}) = \frac{1}{2}\tilde{\mathbf{x}}^T\tilde{\mathbf{Q}}\tilde{\mathbf{x}}$.

In order to shape the closed-loop energy function, we need to relate the state of the controller ξ to the state of the system $\mathbf{x}$. We define the Casimir functions as follows

$$C(\mathbf{x}, \xi) = F(\mathbf{x}) - \xi. \tag{48}$$

These Casimirs functions are invariant quantities along the closed-loop system trajectories independent from the energy function H_d, *i.e.*,

$$\dot{C}(\mathbf{x}, \xi) = \begin{bmatrix} \frac{\partial^T F}{\partial \mathbf{x}} & -I \end{bmatrix} \begin{bmatrix} \mathbf{J} & -\tilde{B}_M^3 g_c^T \\ g_c\tilde{B}_M^{3T} & J_c - R_c \end{bmatrix} \begin{bmatrix} \frac{\partial H_d}{\partial \mathbf{x}}(\mathbf{x}) \\ \frac{\partial H_d}{\partial \xi}(\xi) \end{bmatrix} = 0 \tag{49}$$

which implies the following matching equations:

$$\frac{\partial^T F}{\partial \mathbf{x}}(\mathbf{x})\mathbf{J}\frac{\partial F}{\partial \mathbf{x}}(\mathbf{x}) = J_c(\xi) \tag{50}$$

$$R_c = 0 \tag{51}$$

$$\frac{\partial^T F}{\partial \mathbf{x}}(\mathbf{x})\mathbf{J} = g_c\tilde{B}_M^{3T} \tag{52}$$

Notice that the system (41) does not have dissipation, hence the dissipation obstacle [Ortega et al., 2001] is not occurring. Developing the matching equations (52) we obtain:

$$\frac{\partial^T F}{\partial \mathbf{x}_1}\tilde{T}_{1M} = \frac{\partial^T F}{\partial \mathbf{x}_1}\tilde{T}_{2M} = 0 \tag{53}$$

$$\frac{\partial^T F}{\partial \mathbf{x}_2}\tilde{T}_{1M}^T + \frac{\partial^T F}{\partial \mathbf{x}_3}\tilde{T}_{2M}^T = g_c\tilde{B}_M^{3T} \tag{54}$$

From the equations (53), we can see the function $F(\mathbf{x})$ does not depend on the variables $\mathbf{x}_1$. Taking $g_c = I$ and the matrices defined in (41), a possible solution of the matching condition is:

$$F(\mathbf{x}) = \frac{1}{2}\tilde{B}_M^3 \tilde{T}_{1M}^{-1}\mathbf{x}_2 + \frac{1}{2}\tilde{B}_M^3 \tilde{T}_{2M}^{-1}\mathbf{x}_3 \tag{55}$$

A simple choice for the Casimir function is $C(\mathbf{x},\xi) = C(\mathbf{x}_0,\xi_0) = 0$ which implies the the following relation between the system and the controller states:

$$\xi = F(\mathbf{x}) = \frac{1}{2}\tilde{B}_M^3 \tilde{T}_{1M}^{-1}\mathbf{x}_2 + \frac{1}{2}\tilde{B}_M^3 \tilde{T}_{2M}^{-1}\mathbf{x}_3 \tag{56}$$

The state of the controller is related to $\mathbf{x}_2$, $\mathbf{x}_3$, hence the energy can be shaped in these coordinates. To this end define the Hamiltonian of the controller as

$$H_c(\xi) = 2K\xi^2 \tag{57}$$

This Hamiltonian allows to shape the energy H_d around the zero equilibrium position with $K > 0$ a control design parameter. Following the matching equations (50) and (51), the matrices $J_c = R_c = 0$ and $g_c = I$. Then the controller is:

$$\begin{aligned} \dot{\xi} &= u_c \\ y_c &= \tfrac{\partial H_c}{\partial \xi} \end{aligned} \tag{58}$$

Using this controller, we can shape the energy in the y direction through the local actuation.

Considering (56), the Hamiltonian of the controller can be written as :

$$H_c(\mathbf{x}_2,\mathbf{x}_2) = \frac{1}{2}\mathbf{x}_2^T S_{c2}\mathbf{x}_2 + \frac{1}{2}\mathbf{x}_3^T S_{c3}\mathbf{x}_3 + \mathbf{x}_2^T S_{c4}\mathbf{x}_3 \tag{59}$$

where $S_{c2} = \tilde{T}_{1M}^{-T}\tilde{B}_M^{3T}K\tilde{B}_M^3\tilde{T}_{1M}^{-1}$, $S_{c3} = \tilde{T}_{2M}^{-T}\tilde{B}_M^{3T}K\tilde{B}_M^3\tilde{T}_{1M}^{-2}$, $S_{c4} = \tilde{T}_{1M}^{-T}\tilde{B}_M^{3T}K\tilde{B}_M^3\tilde{T}_{2M}^{-1}$.

From (58), (56) and (47), the control law can be written as:

$$u = -y_c = -2K\tilde{B}_M^3\tilde{T}_{1M}^{-1}\mathbf{x}_2 - 2K\tilde{B}_M^3\tilde{T}_{2M}^{-1}\mathbf{x}_3 \tag{60}$$

with closed loop Hamiltonian

$$H_d = \frac{1}{2}\mathbf{x}_1^T S_1\mathbf{x}_1 + \frac{1}{2}\mathbf{x}_2^T \bar{S}_2\mathbf{x}_2 + \frac{1}{2}\mathbf{x}_3^T \bar{S}_3\mathbf{x}_3 + \mathbf{x}_2^T S_{c4}\mathbf{x}_3 \tag{61}$$

with $\bar{S}_2 = S_2 + S_{c2}$, $\bar{S}_3 = S_3 + S_{c3}$. Furthermore, by adding a negative output feedback to the boundary feedback we introduce dissipation into the closed-loop system and guarantee the closed-loop asymptotic stability [Macchelli et al., 2017]:

$$u^* = u - \alpha y_s \tag{62}$$

with the dissipation feedback coefficient $\alpha > 0$.

5. Numerical simulations

In order to illustrate the numerical effectiveness of the proposed discretization scheme and the simple control strategy, we simulate the 2D wave propagation in the vibro-acoustic tube with the numerical parameters given in Table 1 [David et al., 2010].

Table 1. The parameters of the experimental tube

L	Length	$1.84\ m$
R	Radius	$0.05\ m$
ρ	Air density	$0.8163\ kg/m^3$
χ_s	Compressibility coefficient	$1.4161 \times 10^5\ Pa^{-1}$

We apply the previously proposed discretization scheme using 5 vertical elements *i.e.*, $N = 5$ and 250 horizontal elements *i.e.*, $M = 250$. Hence, the overall system has $M \times N = 1250$ elements and 3750 state variables $\tilde{\mathbf{x}} \in \mathbb{R}^{3750}$. The input is the wave pressure on the left side of the tube generated by the loudspeaker in sinusoidal form $u = \sin(100 * t)$. In Fig. 5, we show the open loop response of the pressure on the complete spatial domain after 5 second.

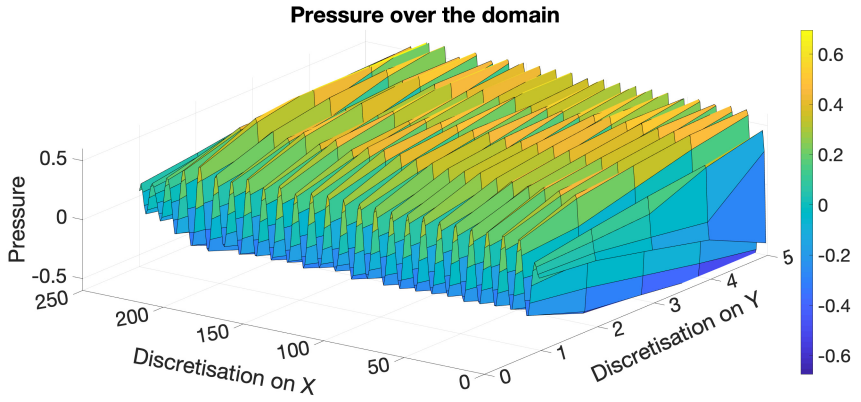

FIG. 5. Open loop pressure response over the 2D domain at 0.5 s

In Fig. 6, the closed-loop response with the passive controller proposed in the last section is shown. To illustrate the effectiveness of the proposed control, we consider the first section of the tube (first 100th elements) is not actuated and that the control action stars from the element 100 to the end. The pressure over the spatial domain at 5 second is shown in Fig. 6. We observe that until the 100th element, the wave is not attenuated. However, starting from element 101 the pressure is attenuated significantly because of the controller. The 2D simulation result confirms the preliminary results proposed in the 1D scenario in [Trenchant et al., 2017b].

6. Conclusion

A geometric structure-preserving discretization for a 2D vibro-acoustic system under the port-Hamiltonian form is addressed in this paper. With a precise choice of a set of basis functions, a finite-dimensional Dirac structure is derived using a mixed finite-elements method and an explicit input-output system representation of the vibro-acoustic tube is achieved. The advantage is that, in the finite dimensional

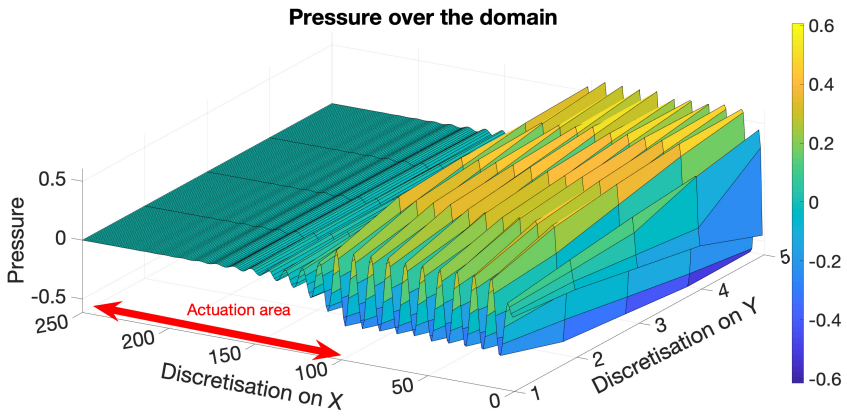

FIG. 6. Closed-loop pressure response over the 2D domain at 0.5 s

approximation of the vibro-acoustic system, the passivity and the Hamiltonian structure is preserved which is useful for control design. Furthermore, a passive controller via interconnection energy shaping and damping injection is implemented on the obtained finite dimensional approximation. The numerical result shows the effectiveness of the proposed discretization scheme and the passive controller. In this paper, we consider a local energy shaping control through the vertical direction, the ongoing work is to design the controller to account for the horizontal structure of the vibro-acoustic tube. The other ongoing work is on the implementation of the proposed controller on real experimental set-up.

Acknowledgment

This work was supported by the ANR-DFG (French-German) project INFIDHEM (contract "ANR-16-CE92-0028"), the Labex ACTION project (contract "ANR-11-LABX-0001-01") and the Bourgogne-Franche-comté Region ANER project (contract "2018Y-06145"). The third author would like to thank the AC3E BASAL project under the reference FB0008 and FONDECYT 1191544.

References

A. Baaiu, F. Couenne, Y. Le Gorrec, L. Lefèvre, and M. Tayakout. Structure-preserving infinite dimensional model reduction application to adsorption processes. *Journal of Process Control*, 19(3): 394–404, 2009.

A. Brugnoli, D. Alazard, V. Pommier-Budinger, and D. Matignon. Port-hamiltonian formulation and symplectic discretization of plate models part i: Mindlin model for thick plates. *Applied Mathematical Modelling*, 75:940 – 960, 2019a. ISSN 0307-904X.

A. Brugnoli, D. Alazard, V. Pommier-Budinger, and D. Matignon. Port-hamiltonian formulation and symplectic discretization of plate models part ii: Kirchhoff model for thin plates. *Applied Mathematical Modelling*, 75:961 – 981, 2019b. ISSN 0307-904X.

F.L. Cardoso-Ribeiro, D. Matignon, and L. Lefèvre. A structure-preserving partitioned finite element method for the 2d wave equation. *IFAC-PapersOnLine*, 51(3):119 – 124, 2018. ISSN 2405-8963. 6th IFAC Workshop on Lagrangian and Hamiltonian Methods for Nonlinear Control LHMNC 2018.

P. David, M. Collet, and J.-M. Cote. Experimental implementation of acoustic impedance control by a 2d network of distributed smart cells. *Smart Materials and Structures*, 19(3):035028, 2010.

V. Duindam, A. Macchelli, S. Stramigioli, and H. eds. Bruyninckx. *Modeling and Control of Complex Physical Systems - The Port-Hamiltonian Approach*. Springer, Sept. 2009. ISBN 978-3-642-03195-3.

J.-F. Durand, C. Soize, and L. Gagliardini. Structural-acoustic modeling of automotive vehicles in presence of uncertainties and experimental identification and validation. *Journal of the Acoustical Society of America*, 124(3):Pages: 1513–1525, 2008.

P. Gardonio. Review of Active Techniques for Aerospace Vibro-Acoustic Control. *Journal of Aircraft*, 39:206–214, 2002.

G. Golo, V. Talasila, A.J. van der Schaft, and B.M. Maschke. Hamiltonian Discretization of Boundary Control Systems. *Automatica*, 40:757–771, 2004.

P. Kotyczka. Finite volume structure-preserving discretization of 1d distributed-parameter port-hamiltonian systems. *IFAC-PapersOnLine*, 49(8):298 – 303, 2016. ISSN 2405-8963. 2nd IFAC Workshop on Control of Systems Governed by Partial Differential Equations CPDE 2016.

P. Kotyczka and B. Maschke. Discrete port-Hamiltonian formulation and numerical approximation for systems of two conservation laws. *at - Automatisierungstechnik*, 65(5):pp. 308–322, May 2017.

P. Kotyczka, B. Maschke, and L. Lefèvre. Weak form of Stokes Dirac structures and geometric discretization of port-hamiltonian systems. *Journal of Computational Physics*, 361:442 – 476, 2018. ISSN 0021-9991.

Y. Le Gorrec, H. Zwart, and B. Maschke. Dirac Structures and Boundary Control Systems Associated with Skew-symmetric Differential Operators. *SIAM Journal on Control and Optimization*, 44:1864–1892, 2005.

A. Macchelli, Y. Le Gorrec, H. Ramírez, and H. Zwart. On the synthesis of boundary control laws for distributed port-hamiltonian systems. *IEEE Transactions on Automatic Control*, 62(4):1700–1713, 2017.

R. Moulla, L. Lefèvre, and B. Maschke. Pseudo-spectral methods for the spatial symplectic reduction of open systems of conservation laws. *Journal of computational Physics*, 231:1272–1292, 2011.

R. Ortega, A.J. van der Schaft, I. Mareels, and B. Maschke. Putting energy back in control. *IEEE Control Systems Magazine*, 21(2):18– 32, April 2001.

A. Serhani, D. Matignon, and G. Haine. Structure-preserving finite volume method for 2d linear and non-linear port-hamiltonian systems. *IFAC-PapersOnLine*, 51(3):131 – 136, 2018. ISSN 2405-8963. 6th IFAC Workshop on Lagrangian and Hamiltonian Methods for Nonlinear Control LHMNC 2018.

M. Seslija, A. van der Schaft, and J. Scherpen. Discrete exterior geometry approach to structure-preserving discretization of distributed-parameter port-Hamiltonian systems. *Journal of Geometry and Physics*, 62(6):1509–1531, 2012.

N.M. Trang Vu, L. Lefèvre, R. Nouailletas, and S. Bremond. Symplectic spatial integration schemes for systems of balance equations. *Journal of Process Control*, 51:1 – 17, 2017. ISSN 0959-1524.

N.M Trang Vu, L. Lefèvre, and B. Maschke. Geometric spatial reduction for port-hamiltonian systems. *Systems & Control Letters*, 125:1 – 8, 2019. ISSN 0167-6911.

V. Trenchant, Y. Fares, H. Ramirez, and Y. Le Gorrec. A port-hamiltonian formulation of a 2d boundary controlled acoustic system. *IFAC-PapersOnLine*, 48(13):235 – 240, 2015. ISSN 2405-8963. 5th IFAC Workshop on Lagrangian and Hamiltonian Methods for Nonlinear Control LHMNC 2015.

V. Trenchant, H. Ramirez, Y. Le Gorrec, and P. Kotyczka. Structure preserving spatial discretization of 2d hyperbolic systems using staggered grids finite difference. In *2017 American Control Conference (ACC)*, pages 2491–2496, May 2017a.

V. Trenchant, T. Vu, H. Ramirez, L. Lefèvre, and Y. Le Gorrec. On the use of structural invariants for the distributed control of infinite dimensional port-hamitonian systems. In *2017 IEEE 56th Annual Conference on Decision and Control (CDC)*, pages 47–52, Dec 2017b.

V. Trenchant, W. Hu, H. Ramirez, and Y. Le Gorrec. Structure preserving finite differences in polar coordinates for heat and wave equations. *IFAC-PapersOnLine*, 51(2):571 – 576, 2018a. ISSN 2405-8963. 9th Vienna International Conference on Mathematical Modelling.

V. Trenchant, H. Ramirez, Y. Le Gorrec, and P. Kotyczka. Finite differences on staggered grids preserving the port-hamiltonian structure with application to an acoustic duct. *Journal of Computational Physics*, 373:673 – 697, 2018b. ISSN 0021-9991.

A.J. van der Schaft. *L_2-gain and Passivity Techniques in Nonlinear Control*. Communications and Control Engineering Series. Springer-Verlag, 2000. ISBN 9781852330736.

A.J. van der Schaft and B. Maschke. Hamiltonian Formulation of Distributed Parameter Systems with Boundary Energy Flow. *Journal of Geometry and Physics*, 42:166–194, 2002.

Y. Wu, B. Hamroun, Y. Le Gorrec, and B. Maschke. Power preserving model reduction of 2d vibro-acoustic system: A port hamiltonian approach. *IFAC-PapersOnLine*, 48(13):206 – 211, 2015. ISSN 2405-8963. 5th IFAC Workshop on Lagrangian and Hamiltonian Methods for Nonlinear Control LHMNC 2015.

Appendix 1: Finite dimensional Dirac structure approximation of a square grid

In this section, we deduce the finite dimensional Dirac structure for a square grid. Substituting compatibility conditions (19) into equations (17) and (18) and integrating over $\mathscr{Z}_{abcd}$, the relations between the approximated flow and effort variables are given by:

$$\begin{aligned} f^{\theta}_{ab} &= e^{p}_{a} - e^{p}_{b}, \quad f^{\theta}_{bc} = e^{p}_{b} - e^{p}_{c}, \\ f^{\theta}_{cd} &= e^{p}_{c} - e^{p}_{c}, \quad f^{\theta}_{da} = e^{p}_{d} - e^{p}_{a}. \end{aligned} \tag{63}$$

$$f^{\Gamma}_{abcd} = e^{v}_{ab} + e^{v}_{bc} + e^{\mathrm{v}}_{cd} + e^{v}_{da} \tag{64}$$

The objective here is to get a finite dimensional system with port-Hamiltonian structure which guarantees the energy balance. To do so, we compute the net power over a square grid *abcd* $P^{net}_{abcd} =$

$P^{\theta}_{abcd} + P^{\Gamma}_{abcd} + P^{B}_{abcd}$ composed of the kinetic power, the potential power and the power through the boundary.

The potential power over a square grid is computed by using the approximated variables and compatibility conditions as:

$$P^{\Gamma}_{abcd} = \int_{\mathscr{Z}_{abcd}} e^{p}(t,z) \wedge f^{\Gamma}(t,z) = f^{\Gamma}_{abcd} e^{\Gamma}_{abcd} \tag{65}$$

where $e^{\Gamma}_{abcd} = \alpha_a e^{p}_{a} + \alpha_b e^{p}_{b} + \alpha_c e^{p}_{c} + \alpha_d e^{p}_{d}$ and

$$\alpha_m \coloneqq \int_{\mathscr{Z}_{abcd}} w^{p}_{m} \wedge w^{\Gamma}_{abcd},\ m \in \{a,b,c,d\}. \tag{66}$$

The kinetic power P^{θ}_{abcd} in the domain can be computed as

$$P^{\theta}_{abcd} = \int_{\mathscr{Z}_{abcd}} e^{v}(t,z) \wedge f^{\theta}(t,z) = f^{\theta}_{ab} e^{\theta}_{ab} + f^{\theta}_{cd} e^{\theta}_{cd} + f^{\theta}_{da} e^{\theta}_{da} \tag{67}$$

with the ports $\left(f^{\theta}_{ab}, e^{\theta}_{ab}\right)$, $\left(f^{\theta}_{cd}, e^{\theta}_{cd}\right)$ and $\left(f^{\theta}_{da}, e^{\theta}_{da}\right)$ identified by

$$\begin{aligned}
e^{\theta}_{ab} &= (\alpha_b - \beta_{b,ab}) e^{v}_{ab} + (\alpha_b - \beta_{b,bc}) e^{v}_{bc} \\
&\quad + (\alpha_b - \beta_{b,cd}) e^{v}_{cd}(t) + (\alpha_b - \beta_{b,da}) e^{v}_{da} \\
e^{\theta}_{cd} &= (\beta_{c,ab} - \alpha_c) e^{v}_{ab} + (\beta_{c,bc} - \alpha_c) e^{v}_{bc} \\
&\quad + (\beta_{c,cd} - \alpha_c) e^{v}_{cd} + (\beta_{c,da} - \alpha_c) e^{v}_{da} \\
e^{\theta}_{da} &= (\beta_{c,ab} + \beta_{d,ab} - \alpha_c - \alpha_d) e^{v}_{ab} \\
&\quad + (\beta_{c,bc} + \beta_{d,bc} - \alpha_c - \alpha_d) e^{v}_{bc} \\
&\quad + (\beta_{c,cd} + \beta_{d,cd} - \alpha_c - \alpha_d) e^{v}_{cd} \\
&\quad + (\beta_{c,da} + \beta_{d,da} - \alpha_c - \alpha_d) e^{v}_{da}
\end{aligned}$$

with α_m defined as (66) and

$$\beta_{m,l} = \int_{\partial \mathscr{Z}_{abcd}} w^{p}_{m} \wedge w^{v}_{l},\ \begin{array}{l} m \in \{a,b,c,d\} \\ l \in \{ab,bc,cd,da\} \end{array}. \tag{68}$$

The power corresponding to the boundary can be computed as follows

$$\begin{aligned}
P^{B}_{abcd} &= \textstyle\int_{\partial \mathscr{Z}_{abcd}} e^{B}(t,z) \wedge f^{B}(t,z) \\
&= e^{B}_{ab} f^{B}_{ab} + e^{B}_{bc} f^{B}_{bc} + e^{B}_{cd} f^{B}_{cd} + e^{B}_{da} f^{B}_{da}
\end{aligned} \tag{69}$$

by identifying the ports on the boundary as $\left(f^{B}_{ab}, e^{B}_{ab}\right)$, $\left(f^{B}_{bc}, e^{B}_{bc}\right)$, $\left(f^{B}_{cd}, e^{B}_{cd}\right)$ and $\left(f^{B}_{da}, e^{B}_{da}\right)$, where

$$\begin{aligned}
e^{B}_{ab} &= \beta_{a,ab} e^{p}_{a} + \beta_{b,ab} e^{p}_{b} + \beta_{c,ab} e^{p}_{c} + \beta_{d,ab} e^{p}_{d} \\
e^{B}_{bc} &= \beta_{a,bc} e^{p}_{a} + \beta_{b,bc} e^{p}_{b} + \beta_{c,bc} e^{p}_{c} + \beta_{d,bc} e^{p}_{d} \\
e^{B}_{cd} &= \beta_{a,cd} e^{p}_{a} + \beta_{b,cd} e^{p}_{b} + \beta_{c,cd} e^{p}_{c} + \beta_{d,cd} e^{p}_{d} \\
e^{B}_{da} &= \beta_{a,da} e^{p}_{a} + \beta_{b,da} e^{p}_{b} + \beta_{c,da} e^{p}_{c} + \beta_{d,da} e^{p}_{d}
\end{aligned}$$

with $\beta_{m,l} = \int_{\partial \mathscr{Z}_{abcd}} w^{v}_{m} \wedge w^{p}_{l}$, $m \in \{a,b,c,d\}$ and $l \in \{ab,bc,cd,da\}$.

Using the net power relations (67), (65) and (69), we can write the finite dimensional Dirac structure over each square grid with its image representation [Duindam et al., 2009] as follows

$$\mathscr{D}_{abcd} = \left\{ (f_{abcd}, e_{abcd}) \,\middle|\, \begin{matrix} f_{abcd} = E^*_{abcd}\lambda_{abcd} \\ e_{abcd} = F^*_{abcd}\lambda_{abcd} \end{matrix}, \lambda_{abcd} \in \mathbb{R}^8 \right\} \tag{70}$$

where

$$f_{abcd} = \left[f^{\Gamma}_{abcd}, f^{\theta}_{ab}, f^{\theta}_{cd}, f^{\theta}_{da}, f^{B}_{ab}, f^{B}_{bc}, f^{B}_{cd}, f^{B}_{da} \right]^T \in \mathbb{R}^8,$$

$$e_{abcd} = \left[e^{\Gamma}_{abcd}, e^{\theta}_{ab}, e^{\theta}_{cd}, e^{\theta}_{da}, e^{B}_{ab}, -e^{B}_{bc}, -e^{B}_{cd}, e^{B}_{da} \right]^T \in \mathbb{R}^8,$$

$$\lambda_{abcd} = \left[e^{p}_{a}, e^{p}_{b}, e^{p}_{c}, e^{p}_{d}, e^{v}_{ab}, e^{v}_{bc}, e^{v}_{cd}, e^{v}_{da} \right]^T \in \mathbb{R}^8$$

and the matrices E_{abcd} and F_{abcd} are define by

$$E^*_{abcd} = \begin{bmatrix} 0 & 0 & 0 & 0 & 1 & 1 & 1 & 1 \\ 1 & -1 & 0 & 0 & 0 & 0 & 0 & 0 \\ 0 & 0 & 1 & -1 & 0 & 0 & 0 & 0 \\ -1 & 0 & 0 & 1 & 0 & 0 & 0 & 0 \\ 0 & 0 & 0 & 0 & 1 & 0 & 0 & 0 \\ 0 & 0 & 0 & 0 & 0 & 1 & 0 & 0 \\ 0 & 0 & 0 & 0 & 0 & 0 & 1 & 0 \\ 0 & 0 & 0 & 0 & 0 & 0 & 0 & 1 \end{bmatrix} \tag{71}$$

$$F^*_{abcd} = \begin{bmatrix} \alpha_a & \alpha_b & \alpha_c & \alpha_d & 0 & 0 & 0 & 0 \\ 0 & 0 & 0 & 0 & \gamma_{b,ab} & \gamma_{b,bc} & \gamma_{b,cd} & \gamma_{b,da} \\ 0 & 0 & 0 & 0 & -\gamma_{c,ab} & -\gamma_{c,bc} & -\gamma_{c,cd} & -\gamma_{c,da} \\ 0 & 0 & 0 & 0 & \gamma_{ab} & \gamma_{bc} & \gamma_{cd} & \gamma_{da} \\ \beta_{a,ab} & \beta_{b,ab} & \beta_{c,ab} & \beta_{d,ab} & 0 & 0 & 0 & 0 \\ \beta_{a,bc} & \beta_{b,bc} & \beta_{c,bc} & \beta_{d,bc} & 0 & 0 & 0 & 0 \\ \beta_{a,cd} & \beta_{b,cd} & \beta_{c,cd} & \beta_{d,cd} & 0 & 0 & 0 & 0 \\ \beta_{a,da} & \beta_{b,da} & \beta_{c,da} & \beta_{d,da} & 0 & 0 & 0 & 0 \end{bmatrix} \tag{72}$$

with $\gamma_{m,l} = \alpha_m - \beta_{m,l}$, $\gamma_l = \beta_l - \alpha_{cd}$, $\alpha_{cd} = \alpha_c + \alpha_d$, $\beta_l = \beta_{c,l} + \beta_{d,l}$, $m \in \{a,b,c,d\}$, and $l \in \{ab,bc,cd,da\}$.

Using the basis function (20)-(22), the parameters α and β can be computed as follows:

$$\begin{aligned} \alpha_{a,abcd} &= \textstyle\int_{z_{abcd}} w_a \wedge w_{abcd} \\ &= \textstyle\int_{y_1}^{y_2} \int_{x_1}^{x_2} \frac{(x_2-x)}{(x_2-x_1)} \frac{(y_2-y)}{(y_2-y_1)} \frac{1}{(x_2-x_1)(y_2-y_1)} dx \wedge dy \\ &= \tfrac{1}{4}. \end{aligned} \tag{73}$$

By doing the same computation, one can find $\alpha_{a,abcd} = \alpha_{b,abcd} = \alpha_{c,abcd} = \alpha_{d,abcd} = \frac{1}{4}$ and

$$\begin{aligned} \beta_{a,ab} &= \textstyle\int_{\partial z_{abcd}} w_a \wedge w_{ab} \\ &= \textstyle\int_{x_1}^{x_2} \frac{(x_2-x)}{(x_2-x_1)} \frac{(y_2-y)}{(y_2-y_1)} \frac{(y_2-y)}{(x_2-x_1)(y_2-y_1)} dx \Big|_{y=y_1} \\ &= \tfrac{1}{2}. \end{aligned} \tag{74}$$

In the same way:

$$\begin{array}{llll} \beta_{a,ab}=\frac{1}{2}, & \beta_{b,ab}=\frac{1}{2}, & \beta_{c,ab}=0, & \beta_{d,ab}=0, \\ \beta_{a,bc}=0, & \beta_{b,bc}=\frac{1}{2}, & \beta_{c,bc}=\frac{1}{2}, & \beta_{d,bc}=0, \\ \beta_{a,cd}=0, & \beta_{b,cd}=0, & \beta_{c,cd}=\frac{1}{2}, & \beta_{d,cd}=\frac{1}{2}, \\ \beta_{a,da}=\frac{1}{2}, & \beta_{b,da}=0, & \beta_{c,da}=0, & \beta_{d,da}=\frac{1}{2}. \end{array} \tag{75}$$

Furthermore, the following parameters can be computed:

$$\begin{array}{rcl} \alpha_{cd} & = & \alpha_{c,abcd}+\alpha_{d,abcd}=\frac{1}{2} \\ \beta_{ab} & = & \beta_{c,ab}+\beta_{d,ab}=0 \\ \beta_{bc} & = & \beta_{c,bc}+\beta_{d,bc}=\frac{1}{2} \\ \beta_{cd} & = & \beta_{c,cd}+\beta_{d,cd}=1 \\ \beta_{da} & = & \beta_{c,da}+\beta_{d,da}=\frac{1}{2} \end{array} \tag{76}$$

Using the above coefficients, one can get the finite dimensional Dirac structure approximation of the square grid (23).

Appendix 2: Constitutive equations approximation

To construct the explicit finite dimensional approximation of the port-Hamiltonian system on the square grid, we should also derive the approximation of the constitutive relations (9). Now let consider the approximation of the energy variables as:

$$\Gamma(t,z) = \Gamma_{abcd} w^{\Gamma}_{abcd} \tag{77}$$

$$\theta(t,z) = \theta_{ab} w^{\theta}_{ab} + \theta_{bc} w^{\theta}_{bc} + \theta_{cd} w^{\theta}_{cd} + \theta_{da} w^{\theta}_{da} \tag{78}$$

In order to derive the constitutive equations of the finite dimensional approximation, we compute the energy over a square grid with the approximated energy variables. First, we consider the potential energy over the square $\mathscr{Z}_{abcd}$ as

$$\begin{array}{rcl} H^{\Gamma}_{abcd} & = & \frac{1}{2}\int_{\mathscr{Z}_{abcd}} \Gamma(z,t)\wedge *\frac{\Gamma(z,t)}{\rho_0} \\ & = & \frac{\Gamma^2_{abcd}}{2}\int_{\mathscr{Z}_{abcd}} \frac{w^{\Gamma}_{abcd}\wedge *w^{\Gamma}_{abcd}}{\chi_s} = \frac{\Gamma^2_{abcd}}{2\chi} \end{array} \tag{79}$$

with $\chi^{-1}=\int_{\mathscr{Z}_{abcd}} \frac{w^{\Gamma}_{abcd}\wedge *w^{\Gamma}_{abcd}}{\chi_s}$. Then using the basis function (20), one can get:

$$\begin{array}{rcl} \chi^{-1} & = & \int_{\mathscr{Z}_{abcd}} \frac{w^{\Gamma}_{abcd}\wedge *w^{\Gamma}_{abcd}}{\chi_s} \\ & = & \frac{1}{\chi_s}\int_{y_1}^{y_2}\int_{x_1}^{x_2}\left[\frac{1}{(x_2-x_1)(y_2-y_1)}\right]^2 dx\wedge dy \\ & = & \frac{1}{\chi_s}\frac{1}{(x_2-x_1)(y_2-y_1)} = \frac{1}{\chi_s}\frac{1}{R_{inf}L_{inf}} \end{array} \tag{80}$$

where $L_{in}=x_2-x_1$ and $R_{in}=y_2-y_1$ are the length and the width of the square grid respectively.

Before deriving the kinetic energy over the square $\mathscr{Z}_{abcd}$, we rewrite the kinetic momentum by using the compatibility conditions (19) as:

$$\theta(t,z) = \theta_{ab} dw^p_b - \theta_{cd} dw^p_c - \theta_{da}(dw^p_c + dw^p_d). \tag{81}$$

These finite dimensional energy variables has been chosen with respect to the effort variables over the square from the net power balance (67). Using the energy variables defined above, the kinetic energy is expressed as:

$$\begin{aligned} H^{\theta}_{abcd} &= \tfrac{1}{2}\int_{\mathscr{Z}_{abcd}} \theta(z,t)\wedge *\frac{\theta(z,t)}{\rho_0} \\ &= \tfrac{1}{2}\left[\frac{\theta^2_{ab}}{\rho_1}+\frac{\theta^2_{cd}}{\rho_2}+\frac{\theta^2_{da}}{\rho_3}-\frac{2\theta_{ab}\theta_{cd}}{\rho_4}-\frac{2\theta_{ab}\theta_{da}}{\rho_5}+\frac{2\theta_{cd}\theta_{da}}{\rho_6}\right] \end{aligned} \tag{82}$$

with $\rho_1^{-1}=\int_{\mathscr{Z}_{abcd}}\frac{dw_b^p\wedge *dw_b^p}{\rho_0}$, $\rho_2^{-1}=\int_{\mathscr{Z}_{abcd}}\frac{dw_c^p\wedge *dw_c^p}{\rho_0}$, $\rho_3^{-1}=\int_{\mathscr{Z}_{abcd}}\frac{(dw_c^p+dw_d^p)\wedge *(dw_c^p+dw_d^p)}{\rho_0}$,
$\rho_4^{-1}=\int_{\mathscr{Z}_{abcd}}\frac{dw_b^p\wedge *dw_c^p+dw_c^p\wedge *dw_b^p}{2\rho_0}$, $\rho_5^{-1}=\int_{\mathscr{Z}_{abcd}}\frac{dw_b^p\wedge *(dw_c^p+dw_d^p)+(dw_c^p+dw_d^p)\wedge *dw_b^p}{2\rho_0}$,
$\rho_6^{-1}=\int_{\mathscr{Z}_{abcd}}\frac{dw_c^p\wedge *(dw_c^p+dw_d^p)+(dw_c^p+dw_d^p)\wedge *dw_c^p}{2\rho_0}$.

Using the chosen basis functions (22), we can compute the above parameters:

$$\begin{aligned} \rho_1^{-1} &= \frac{1}{3\rho_0}\left[\frac{y_2-y_1}{x_2-x_1}+\frac{x_2-x_1}{y_2-y_1}\right]=\frac{1}{3\rho_0}\left[\frac{R_{in}}{L_{in}}+\frac{L_{in}}{R_{in}}\right], \\ \rho_2^{-1} &= \frac{1}{3\rho_0}\left[\frac{y_2-y_1}{x_2-x_1}+\frac{x_2-x_1}{y_2-y_1}\right]=\frac{1}{3\rho_0}\left[\frac{R_{in}}{L_{in}}+\frac{L_{in}}{R_{in}}\right], \\ \rho_3^{-1} &= \frac{1}{\rho_0}\frac{x_2-x_1}{y_2-y_1}=\frac{1}{\rho_0}\frac{L_{in}}{R_{in}}, \\ \rho_4^{-1} &= \frac{1}{3\rho_0}\left[\frac{y_2-y_1}{x_2-x_1}+\frac{x_2-x_1}{y_2-y_1}\right]=\frac{1}{3\rho_0}\left[\frac{R_{in}}{L_{in}}+\frac{L_{in}}{R_{in}}\right], \\ \rho_5^{-1} &= \frac{1}{6\rho_0}\frac{x_2-x_1}{y_2-y_1}=\frac{1}{6\rho_0}\frac{L_{in}}{R_{in}}, \\ \rho_6^{-1} &= \frac{1}{2\rho_0}\frac{x_2-x_1}{y_2-y_1}=\frac{1}{2\rho_0}\frac{L_{in}}{R_{in}}. \end{aligned} \tag{83}$$

The finite dimensional approximation of the constitutive relations can be written as

$$\begin{bmatrix} e^{\Gamma}_{abcd} \\ e^{\theta}_{ab} \\ e^{\theta}_{cd} \\ e^{\theta}_{da} \end{bmatrix} = Q_{abcd}\begin{bmatrix} \Gamma_{abcd} \\ \theta_{ab} \\ \theta_{cd} \\ \theta_{da} \end{bmatrix} \tag{84}$$

with

$$Q_{abcd}=\begin{bmatrix} S_{in}\frac{1}{\chi_s} & 0 & 0 & 0 \\ 0 & \frac{1}{3}S_{2in}\frac{1}{\rho_0} & -\frac{1}{3}S_{2in}\frac{1}{\rho_0} & -S_{1in}\frac{1}{6\rho_0} \\ 0 & -\frac{1}{3}S_{2in}\frac{1}{\rho_0} & \frac{1}{3}S_{2in}\frac{1}{\rho_0} & S_{1in}\frac{1}{2\rho_0} \\ 0 & -S_{1in}\frac{1}{6\rho_0} & S_{1in}\frac{1}{2\rho_0} & S_{1in}\frac{1}{\rho_0} \end{bmatrix}. \tag{85}$$

and $S_{in}=\frac{1}{L_{in}R_{in}}$, $S_{1in}=\frac{R_{in}}{L_{in}}$ and $S_{2in}=\frac{R_{in}}{L_{in}}+\frac{L_{in}}{R_{in}}$.